Atmos. Chem. Phys. Discuss., https://doi.org/10.5194/acp-2018-385
Manuscript under review for journal Atmos. Chem. Phys.
Discussion started: 8 May 2018
© Author(s) 2018. CC BY 4.0 License.

Atmospheric Chemistry and Physics Discussions

Nitrogen isotope fractionation during gas-particle conversion of NO_x to NO_3^- in the atmosphere – implications for isotope-based NO_x source apportionment

Yunhua Chang[1], Yanlin Zhang[1*], Chongguo Tian[2], Shichun Zhang[3], Xiaoyan Ma[4], Fang Cao[1], Xiaoyan Liu[1], Wenqi Zhang[1], Thomas Kuhn[5], and Moritz F. Lehmann[5]

[1]Yale-NUIST Center on Atmospheric Environment, Nanjing University of Information Science and Technology, Nanjing 10044, China

[2]Key Laboratory of Coastal Environmental Processes and Ecological Remediation, Yantai Institute of Coastal Zone Research, Chinese Academy of Sciences, Yantai 264003, China

[3]Northeast Institute of Geography and Agroecology, Chinese Academy of Sciences, 4888 Shengbei Road, Changchun 130102, China

[4]Key Laboratory for Aerosol Cloud-Precipitation of China Meteorological Administration, Earth System Modeling Center, Nanjing University of Information Science and Technology, Nanjing 10044, China

[5]Aquatic and Isotope Biogeochemistry, Department of Environmental Sciences, University of Basel, Basel 4056, Switzerland

[*] Corresponding author: Yanlin Zhang

E-mail address: dryanlinzhang@outlook.com

Atmos. Chem. Phys. Discuss., https://doi.org/10.5194/acp-2018-385
Manuscript under review for journal Atmos. Chem. Phys.
Discussion started: 8 May 2018
© Author(s) 2018. CC BY 4.0 License.

Atmospheric Chemistry and Physics Discussions

Abstract

Atmospheric fine-particle ($PM_{2.5}$) pollution is frequently associated with the formation of particulate nitrate (pNO_3^-), the end product of the oxidation of NO_x gases (=NO+NO_2) in the upper troposphere. The application of stable nitrogen (N) (and oxygen) isotope analyses of pNO_3^- to constrain NO_x source partitioning in the atmosphere requires the knowledge of the isotope fractionation during the reactions leading to nitrate formation. Here we determined the $\delta^{15}N$ values of fresh pNO_3^- ($\delta^{15}N$-pNO_3^-) in $PM_{2.5}$ at a rural site in Northern China, where atmospheric pNO_3^- can be attributed exclusively to biomass burning. The observed $\delta^{15}N$-pNO_3^- (12.17±1.55‰; n=8) was much higher than the N isotopic source signature of NO_x from biomass burning (1.04±4.13‰). The large difference between $\delta^{15}N$-pNO_3^- and $\delta^{15}N$-NO_x ($\Delta(\delta^{15}N)$) can be reconciled by the net N isotope effect (ε_N) associated with the gas-particle conversion from NO_x to NO_3^-. For the biomass-burning site, a mean ε_N ($\approx \Delta(\delta^{15}N)$) of 10.99±0.74‰ was assessed through a newly-developed computational quantum chemistry (CQC) module. ε_N depends on the relative importance of the two dominant N isotope exchange reactions involved (NO_2 reaction with OH versus hydrolysis of dinitrogen pentoxide (N_2O_5) with H_2O), and varies between regions, and on a diurnal basis. A second, slightly higher CQC-based mean value for ε_N (15.33±4.90‰) was estimated for an urban site with intense traffic in Eastern China, and integrated in a Bayesian isotope mixing model to make isotope-based source apportionment estimates for NO_x at this site. Based on the $\delta^{15}N$ values (10.93±3.32‰, n=43) of ambient pNO_3^- determined for the urban site, and considering the location-specific estimate for ε_N, our results reveal that the relative contribution of coal combustion and road traffic to urban NO_x are 32 ±11% and 68 ±11%, respectively. This finding agrees well with a regional bottom-up emission inventory of NO_x. Moreover, the variation pattern of OH contribution to ambient pNO_3^- formation calculated by the CQC module is consistent with that simulated by the Weather Research and Forecasting model coupled with Chemistry (WRF-Chem), further confirming the robustness of our estimates. Our investigations also show that, without the consideration of the N isotope effect during pNO_3^- formation, the observed $\delta^{15}N$-

Atmos. Chem. Phys. Discuss., https://doi.org/10.5194/acp-2018-385
Manuscript under review for journal Atmos. Chem. Phys.
Discussion started: 8 May 2018
© Author(s) 2018. CC BY 4.0 License.

Atmospheric Chemistry and Physics Discussions

52 $p\mathrm{NO_3^-}$ at the study site would erroneously imply that $\mathrm{NO_x}$ is derived almost entirely
53 from coal combustion. Similarly, reanalysis of reported $\delta^{15}\mathrm{N\text{-}NO_3^-}$ data throughout
54 China and its neighboring areas suggests that, nationwide, $\mathrm{NO_x}$ emissions from coal
55 combustion may be substantively overestimated (by >30%) when the N isotope
56 fractionation during atmospheric $p\mathrm{NO_3^-}$ formation is neglected.

57 **1 Introduction**

58 Nitrogen oxides ($\mathrm{NO_x}$ = NO + $\mathrm{NO_2}$) are among the most important molecules in
59 tropospheric chemistry. They are involved in the formation of secondary aerosols and
60 atmospheric oxidants, such as ozone ($\mathrm{O_3}$) and hydroxyl radicals (OH), which controls
61 the self-cleansing capacity of the atmosphere (Galloway et al., 2003; Seinfeld and
62 Pandis, 2012; Solomon et al., 2007). The sources of $\mathrm{NO_x}$ include both anthropogenic
63 and natural origins, with more than half of the global burden (~40 Tg N $\mathrm{yr^{-1}}$) currently
64 attributed to fossil fuel burning (22.4-26.1 Tg N $\mathrm{yr^{-1}}$) and the rest primarily derived
65 from nitrification/denitrification in soils (including wetlands; 8.9 ± 1.9 Tg N $\mathrm{yr^{-1}}$),
66 biomass burning (5.8 ± 1.8 Tg N $\mathrm{yr^{-1}}$), lightning (2-6 Tg N $\mathrm{yr^{-1}}$), and oxidation of $\mathrm{N_2O}$
67 in the stratosphere (0.1-0.6 Tg N $\mathrm{yr^{-1}}$) (Jaegle et al., 2005; Richter et al., 2005; Lamsal
68 et al., 2011; Price et al., 1997; Yienger and Levy, 1995; Miyazaki et al., 2017; Duncan
69 et al., 2016; Anenberg et al., 2017; Levy et al., 1996). The main/ultimate sinks for
70 $\mathrm{NO_x}$ in the troposphere are the oxidation to nitric acid ($\mathrm{HNO_{3(g)}}$) and the formation of
71 aerosol-phase particulate nitrate ($p\mathrm{NO_3^-}$) (Seinfeld and Pandis, 2012), the partitioning
72 of which may vary on diurnal and seasonal time scales (Morino et al., 2006).

73 Emissions of $\mathrm{NO_x}$ occur mostly in the form of NO (Seinfeld and Pandis, 2012; Leighton,
74 1961). During daytime, transformation from NO to $\mathrm{NO_2}$ is rapid (few minutes) and
75 proceeds in a photochemical steady state, controlled by the oxidation of NO by $\mathrm{O_3}$ to
76 $\mathrm{NO_2}$, and the photolysis of $\mathrm{NO_2}$ back to NO (Leighton, 1961):

77 (R1) $\mathrm{NO + O_3 \longrightarrow NO_2 + O_2}$

78 (R2) $\mathrm{NO_2 + h\nu \longrightarrow NO + O}$

Atmos. Chem. Phys. Discuss., https://doi.org/10.5194/acp-2018-385
Manuscript under review for journal Atmos. Chem. Phys.
Discussion started: 8 May 2018
© Author(s) 2018. CC BY 4.0 License.

Atmospheric Chemistry and Physics Discussions

(R3) $O + O_2 \xrightarrow{M} O_3$,

where M is any non-reactive species that can take up the energy released to stabilize O. NO_x oxidation to HNO_3 is governed by the following equations. During daytime:

(R4) $NO_2 + OH \xrightarrow{M} HNO_3$,

and during nighttime:

(R5) $NO_2 + O_3 \longrightarrow NO_3 + O_2$

(R6) $NO_3 + NO_2 \xrightarrow{M} N_2O_5$

(R7) $N_2O_5 + H_2O_{(surface)} \xrightarrow{aerosol} 2HNO_3$.

HNO_3 then reacts with gas-phase NH_3 to form ammonium nitrate (NH_4NO_3) aerosols. If the ambient relative humidity (RH) is lower than the efflorescence relative humidity (ERH) or crystallization relative humidity (CRH), solid-phase NH_4NO_3(s) is formed (Smith et al., 2012; Ling and Chan, 2007):

(R8a) $NH_4NO_3 \rightleftharpoons HNO_3(g) + NH_3(g)$.

If ambient RH exceeds the ERH or CRH, HNO_3 and NH_3 dissolve into the aqueous phase (aq) (Smith et al., 2012; Ling and Chan, 2007):

(R8b) $HNO_3(g) + NH_3(g) \rightleftharpoons NO_3^-(aq) + NH_4^+(aq)$.

Whilst global NO_x emissions are well constrained, individual source attribution and their local or regional role in particulate nitrate formation are difficult to assess due to the short lifetime of NO_x (typically less than 24 hr), and the high degree of spatiotemporal heterogeneity with regards to the ratio between gas-phase HNO_3 and particulate NO_3^- (pNO_3^-) (Duncan et al., 2016; Lu et al., 2015; Zong et al., 2017; Zhang et al., 2003). Given the conservation of the nitrogen (N) atom between NO_x sources and sinks, the N isotopic composition of pNO_3^- can be related to the different origins of the

Atmos. Chem. Phys. Discuss., https://doi.org/10.5194/acp-2018-385
Manuscript under review for journal Atmos. Chem. Phys.
Discussion started: 8 May 2018
© Author(s) 2018. CC BY 4.0 License.

Atmospheric Chemistry and Physics Discussions

emitted NO_x, and thus provides valuable information on the partitioning of the NO_x sources. Such N isotope balance approach works best if the N isotopic composition of various NO_x sources display distinct $^{15}N/^{14}N$ ratios (reported as $\delta^{15}N=\frac{\left(^{15}N/^{14}N\right)_{sample}-\left(^{15}N/^{14}N\right)_{N_2}}{\left(^{15}N/^{14}N\right)_{N_2}}\times 1000$). The $\delta^{15}N$-NO_x of coal-fired power plant (+10‰ to +25‰) (Felix et al., 2012; Heaton, 1990; Felix et al., 2013), vehicle (+3.7‰ to +5.7‰) (Heaton, 1990; Walters et al., 2015; Felix and Elliott, 2014; Felix et al., 2013; Wojtal et al., 2016), and biomass burning (-7‰ to +12‰) emissions (Fibiger and Hastings, 2016), for example, are generally higher than that of lightning (-0.5‰ to +1.4‰) (Hoering, 1957) and biogenic soil (-48.9‰ to -19.9‰) emissions (Li and Wang, 2008; Felix and Elliott, 2014; Felix et al., 2013), allowing the use of isotope mixing models to gain insight on the NO_x source apportionment for gases, aerosols, as well as the resulting nitrate deposition (-15‰ to +15‰) (Elliott et al., 2007; Zong et al., 2017; Savarino et al., 2007; Morin et al., 2008; Elliott et al., 2009; Park et al., 2018; Altieri et al., 2013; Gobel et al., 2013). In addition, because of mass-independent fractionation during its formation (Thiemens, 1999; Thiemens and Heidenreich, 1983), ozone possesses a strong isotope anomaly ($\Delta^{17}O \approx \delta^{17}O - 0.52*\delta^{18}O$), which is propagated into the most short-lived oxygen-bearing species, including NO_x and nitrate. Therefore, the oxygen isotopic composition of nitrate ($\delta^{18}O$, $\Delta^{17}O$) can provide information on the oxidants involved in the conversion of NO_x to nitrate (Michalski et al., 2003; Geng et al., 2017).

$\delta^{15}N$-based source apportionment of NO_x requires knowledge of how kinetic and equilibrium isotope fractionation may impact $\delta^{15}N$ values during the conversion of NO_x to nitrate (Freyer, 1978; Walters et al., 2016). If these isotope effects are considerable, they may greatly limit the use of $\delta^{15}N$ values of pNO_3^- for NO_x source partition (Walters et al., 2016). Previous studies didn't take into account the potentially biasing effect of N isotope fractionation, because they assumed that changes in the $\delta^{15}N$ values during the conversion of NO_x to nitrate are minor (without detailed explanation) (Kendall et al., 2007; Morin et al., 2008; Elliott et al., 2007) or relatively small (e.g., +3‰) (Felix

© Author(s) 2018. CC BY 4.0 License.

and Elliott, 2014; Freyer, 2017). However, a field study by Freyer et al. (1993) has indicated that N isotope exchange may have a strong influence on the observed $\delta^{15}N$ values in atmospheric NO and NO_2, implying that isotope equilibrium fractionation may play a significant role in shaping the $\delta^{15}N$ of NO_y species (the family of oxidized nitrogen molecules in the atmosphere, including NO_x, NO_3, NO_3^-, peroxyacetyl nitrate etc.). The transformation of NO_x to nitrate is a complex process that involves several different reaction pathways (Walters et al., 2016). To date, few fractionation factors for this conversion have been determined. Recently, Walters and Michalski (2015) and Walters et al. (2016) used computational quantum chemistry methods to calculate N isotope equilibrium fractionation factors for the exchange between major NO_y molecules and confirmed theoretical predictions that ^{15}N isotopes enrich in the more oxidized form of NO_y, and that the transformation of NO_x to atmospheric nitrate (HNO_3, NO_3 (aq), NO_3 (g)) continuously increases the $\delta^{15}N$ in the residual NO_x pool.

As a consequence of its severe atmospheric particle pollution during the cold season, China has made great efforts toward reducing NO_x emissions from on-road traffic (e.g., improving emission standards, higher gasoline quality, vehicle travel restrictions) (Li et al., 2017). Moreover, China has continuously implemented denitrogenation technologies (e.g., selective catalytic reduction or SCR) in the coal-fired power plants sector since the mid-2000s, and has been phasing out small inefficient units (Liu et al., 2015). Monitoring and assessing the efficiency of such mitigation measures, and optimizing policy efforts to further reduce NO_x emissions, requires knowledge of the vehicle- and power plant-emitted NO_x to particulate nitrate in urban China (Ji et al., 2015; Fu et al., 2013; Zong et al., 2017). In this study, the chemical components of ambient fine particles ($PM_{2.5}$) were quantified, and the isotopic composition of particulate nitrate ($\delta^{15}N$-NO_3^-, $\delta^{18}O$-NO_3^-) was assessed in order to elucidate ambient NO_x sources in two distinct areas of China. We also investigated the potential isotope effect during the formation of nitrate aerosols from NO_x, and evaluated how disregard of such N isotope fractionation can bias N-isotope mixing model-based estimates on the NO_x source apportionment for nitrate deposition.

Atmos. Chem. Phys. Discuss., https://doi.org/10.5194/acp-2018-385
Manuscript under review for journal Atmos. Chem. Phys.
Discussion started: 8 May 2018
© Author(s) 2018. CC BY 4.0 License.

Atmospheric Chemistry and Physics Discussions

2 Methods

2.1 Field sampling

In this study, $PM_{2.5}$ aerosol samples were collected on precombusted (450 °C for 6 hr) quartz filters (25 × 20 cm) on a day/night basis, using high-volume air samplers at a flow rate of 1.05 m^3 min^{-1} in Sanjiang and Nanjing (Fig. 1). After sampling, the filters were wrapped in aluminum foil, packed in air-tight polyethylene bags and stored at -20 °C prior to further processing and analysis. Four blank filters were also collected. They were exposed for 10 min to ambient air (i.e., without active sampling). $PM_{2.5}$ mass concentration was analyzed gravimetrically (Sartorius MC5 electronic microbalance) with a ± 1 μg precision before and after sampling (at 25°C and 45 ± 5% during weighing).

Figure 1.

The Sanjiang campaign was performed during a period of intensive burning of agricultural residues between October 8 and 18, 2013, to examine if there is any significant difference between the $\delta^{15}N$ values of pNO_3^- and NO_x emitted from biomass burning. The Sanjiang site (in the following abbreviated as SJ; 47.35°N, 133.31°E) is located at an ecological experimental station affiliated with the Chinese Academy of Sciences located in the Sanjiang Plain, a major agricultural area predominantly run by state farms in Northeastern China (Fig. 1). Surrounded by vast farm fields and bordering Far-Eastern Russia, SJ is situated in a remote and sparsely populated region, with a harsh climate and rather poorly industrialized economy. The annual mean temperature at SJ is close to the freezing point, with daily minima ranging between -31 and -15°C in the coldest month January. As a consequence of the relatively low temperatures (also during summer), biogenic production of NO_x through soil microbial processes is rather

© Author(s) 2018. CC BY 4.0 License.

weak. SJ is therefore an excellent environment where to collect biomass burning-emitted aerosols with only minor influence from other sources.

The Nanjing campaign was conducted between 17 December 2014 and 8 January 2015 with the main objective to examine whether N isotope measurements can be used as a tool to elucidate NO_x source contributions to ambient pNO_3^- during times of severe haze. Situated in the heartland of the lower Yangtze River region, Nanjing is, after Shanghai, the second largest city in Eastern China. The aerosol sampler was placed at the rooftop of a building on the Nanjing University of Information Science and Technology campus (in the following abbreviated as NJ; 18 m a.g.l.; 32.21° N, 118.72° E; Fig. 1), where NO_x emissions derive from both industrial and transportation sources.

2.2 Laboratory analysis

The mass concentrations of inorganic ions (including SO_4^{2-}, NO_3^-, Cl^-, NH_4^+, K^+, Ca^{2+}, Mg^{2+}, and Na^+), carbonaceous components (organic carbon or OC, elemental carbon or EC), and water-soluble organic carbon or WSOC were determined using an ion chromatograph (761 Compact IC, Metrohm, Switzerland), a thermal/optical OC/EC analyzer (RT-4 model, Sunset Lab. Inc., USA), and a TOC analyzer (Shimadzu, TOC-VCSH, Japan), respectively. Importantly, levoglucosan, a molecular marker for the biomass combustion aerosols was detected using a Dionex™ ICS-5000$^+$ system (Thermo Fisher Scientific, Sunnyvale, USA). In addition, a homologous series of dicarboxylic acids (C_2-C_{11}) and related compounds (oxoacids, α-dicarbonyls and fatty acids) were analyzed using an Agilent 7890 gas chromatography and GC-MS detection (Agilent Technologies, Wilmington, USA), employing a dibutyl ester derivatization technique. Chemical aerosol analyses, including sample pre-treatment, analytical procedures, protocol adaption, detection limits, and experimental uncertainty were described in detail in our previous work (Cao et al., 2016; Cao et al., 2017).

For isotopic analyses of aerosol nitrate, aerosol subsamples were generated by punching 1.4-cm disks out of the filters. In order to extract the NO_3^-, sample discs were placed in

Atmos. Chem. Phys. Discuss., https://doi.org/10.5194/acp-2018-385
Manuscript under review for journal Atmos. Chem. Phys.
Discussion started: 8 May 2018
© Author(s) 2018. CC BY 4.0 License.

Atmospheric Chemistry and Physics Discussions

212 acid-washed glass vials with 10 ml deionized water and placed in an ultra-sonic water
213 bath for 30 min. Between one and four disks were used for NO_x extraction, dependent
214 on the aerosol NO_3^- content on the filters, which was determined independently. The
215 extracts were then filtered (0.22 µm) and analyzed the next day. N and O isotope
216 analyses of the extracted/dissolved aerosol nitrate ($^{15}N/^{14}N$, $^{18}O/^{16}O$) were performed
217 using the denitrifier method (Sigman et al., 2001; Casciotti et al., 2002). Briefly, sample
218 NO_3^- is converted to nitrous oxide (N_2O) by denitrifying bacteria that lack N_2O
219 reductase activity (*Pseudomonas chlororaphis* ATCC# 13985; formerly *Pseudomonas*
220 *aureofaciens*, referred to below as such). N_2O is extracted, purified, and analyzed for
221 its N and O isotopic composition using a continuous-flow isotope ratio mass
222 spectrometer (Thermo Finnigan Delta$^+$, Bremen, German). Nitrate N and O isotope
223 ratios are reported in the conventional δ-notation with respect to atmospheric N_2 and
224 standard mean ocean water (V-SMOW) respectively. Analyses are calibrated using the
225 international nitrate isotope standard IAEA-N3, with a $\delta^{15}N$ value of 4.7‰ and a $\delta^{18}O$
226 value of 25.6‰ (Böhlke et al., 2003). The blank contribution was generally lower than
227 0.2 nmol (as compared to 20 nmol of sample N). Based on replicate measurements of
228 standards and samples, the analytical precision for $\delta^{15}N$ and $\delta^{18}O$ was generally better
229 than ± 0.2‰ and ± 0.3‰ (1σ), respectively.

230 The denitrifier method generates $\delta^{15}N$ and $\delta^{18}O$ values of the combined pool of NO_3^-
231 and NO_2^-. The presence of substantial amounts of NO_2^- in NO_3^- samples may lead to
232 errors with regards to the analysis of $\delta^{18}O$ (Wankel et al., 2010). We refrained from
233 including a nitrite-removal step, because nitrite concentrations in our samples were
234 always < 1% of the NO_3^- concentrations. In the following $\delta^{15}N_{NOx}$ and $\delta^{18}O_{NOx}$ are thus
235 referred to as nitrate $\delta^{15}N$ and $\delta^{18}O$ (or $\delta^{15}N_{NO3}$ and $\delta^{18}O_{NO3}$).

236 In the case of atmospheric/aerosol nitrate samples with comparatively high $\delta^{18}O$ values,
237 $\delta^{15}N$ values tend to be overestimated by 1-2‰ (Hastings et al., 2003), if the contribution
238 of $^{14}N^{14}N^{17}O$ to the N_2O mass 45 signal is not accounted for during isotope ratio
239 analysis. For most natural samples, the mass-dependent relationship can be

© Author(s) 2018. CC BY 4.0 License.

approximated as $\delta^{17}O \approx 0.52 \times \delta^{18}O$, and the $\delta^{18}O$ can be used for the ^{17}O correction. Atmospheric NO_3^- does not follow this relationship but inhabits a mass-independent component. Thus, we adopted a correction factor of 0.8 instead of 0.52 for the ^{17}O to ^{18}O linearity (Hastings et al., 2003).

2.3 Calculation of N isotope fractionation value (ε_N)

As we described above, the transformation process of NO_x to HNO_3/NO_3^- involves multiple reaction pathways (see also Fig. S1) and is likely to undergo isotope equilibrium exchange reactions. The measured $\delta^{15}N\text{-}NO_3^-$ values of aerosol samples are thus reflective of the combined N isotope signatures of various NO_x sources ($\delta^{15}N\text{-}NO_x$) plus any given N isotope fractionation. Recently, Walter and Michalski (2015) used a computational quantum chemistry approach to calculate isotope exchange fractionation factors for atmospherically relevant NO_y molecules, and based on this approach, Zong et al. (2017) estimated the N isotope fractionation during the transformation of NO_x to pNO_3^- at a regional background site in China. Here we adopt, and slightly modify, the approach by Walter and Michalski (2015) and Zong et al. (2017), and assumed that the net N isotope effect ε_N (for equilibrium processes A↔B: $\varepsilon_{A\leftrightarrow B} = \left(\frac{(\text{heavy isotope/light isotope})_A}{(\text{heavy isotope/light isotope})_B} - 1\right) \cdot 1000‰$; ε_N refers to $\varepsilon_{N(NO_x\leftrightarrow pNO_3^-)}$ in this study unless otherwise specified) during the gas-to-particle conversion from NO_x to pNO_3^- formation ($\Delta\left(\delta^{15}N\right)_{pNO_3^-\text{-}NO_x} = \delta^{15}N\text{-}pNO_3^- - \delta^{15}N\text{-}NO_x \approx \varepsilon_N$) can be considered a hybrid of the isotope effects of two dominant N isotopic exchange reactions:

$$\begin{aligned}\varepsilon_N &= \gamma \times \varepsilon_{N\left(NO_x\leftrightarrow pNO_3^-\right)_{OH}} + (1-\gamma)\times \varepsilon_{N\left(NO_x\leftrightarrow pNO_3^-\right)_{H_2O}} \\ &= \gamma \times \varepsilon_{N(NO_x\leftrightarrow HNO_3)_{OH}} + (1-\gamma)\times \varepsilon_{N(NO_x\leftrightarrow HNO_3)_{H_2O}}\end{aligned} \quad (1)$$

where γ represents the contribution from isotope fractionation by the reaction of NO_x and photo-chemically produced OH to form HNO_3 (and pNO_3^-), as shown by $\varepsilon_{N(NO_x\leftrightarrow HNO_3)_{OH}}$ ($\varepsilon_{N\left(NO_x\leftrightarrow pNO_3^-\right)_{OH}}$). The remainder is formed by the hydrolysis of N_2O_5

Atmos. Chem. Phys. Discuss., https://doi.org/10.5194/acp-2018-385
Manuscript under review for journal Atmos. Chem. Phys.
Discussion started: 8 May 2018
© Author(s) 2018. CC BY 4.0 License.

Atmospheric Chemistry and Physics Discussions

with aerosol water to generate HNO_3 (and pNO_3^-), namely, $\varepsilon_{N(NO_x \leftrightarrow HNO_3)_{H_2O}}$ ($\varepsilon_{N(NO_x \leftrightarrow pNO_3^-)_{H_2O}}$). Assuming that kinetic N isotope fractionation associated with the reaction between NO_x and OH is negligible, $\varepsilon_{N(NO_x \leftrightarrow pNO_3^-)_{OH}}$ can be calculated based on mass-balance considerations:

$$\varepsilon_{N(NO_x \leftrightarrow pNO_3^-)_{OH}} = \varepsilon_{N(NO_x \leftrightarrow HNO_3)_{OH}} = \varepsilon_{N(NO_2 \leftrightarrow HNO_3)_{OH}} = 1000 \times \left[\frac{\left({}^{15}\alpha_{NO_2/NO} - 1\right)\left(1 - f_{NO_2}\right)}{\left(1 - f_{NO_2}\right) + \left({}^{15}\alpha_{NO_2/NO} \times f_{NO_2}\right)} \right] \quad (2)$$

where ${}^{15}\alpha_{NO_2/NO}$ is the temperature-dependent (see equation 7 and Table S1) equilibrium N isotope fractionation factor between NO_2 and NO, and f_{NO_2} is the fraction of NO_2 in the total NO_x. f_{NO_2} ranges from 0.2 to 0.95 (Walters and Michalski, 2015). Similarly, assuming a negligible kinetic isotope fractionation associated with the reaction $N_2O_5 + H_2O$ + aerosol $\rightarrow 2HNO_3$, $\varepsilon_{N(NO_x \leftrightarrow pNO_3^-)_{H_2O}}$ can be computed from the following equation:

$$\varepsilon_{N(NO_x \leftrightarrow pNO_3^-)_{H_2O}} = \varepsilon_{N(NO_x \leftrightarrow HNO_3)_{H_2O}} = \varepsilon_{N(NO_x \leftrightarrow N_2O_5)_{H_2O}} = 1000 \times \left({}^{15}\alpha_{N_2O_5/NO_2} - 1\right) \quad (3)$$

where ${}^{15}\alpha_{N_2O_5/NO_2}$ is the equilibrium isotope fractionation factor between N_2O_5 and NO_2, which also is temperature-dependent (see equation 7 and Table S1).

Following Walter and Michalski (2015) and Zhong et al. (2017), γ can then be approximated based on the O isotope fractionation during the conversion of NO_x to pNO_3^-:

$$\varepsilon_{O(NO_x \leftrightarrow pNO_3^-)} = \gamma \times \varepsilon_{O(NO_x \leftrightarrow pNO_3^-)_{OH}} + (1-\gamma) \times \varepsilon_{O(NO_x \leftrightarrow pNO_3^-)_{H_2O}} = \gamma \times \varepsilon_{O(NO_x \leftrightarrow HNO_3)_{OH}} + (1-\gamma) \times \varepsilon_{O(NO_x \leftrightarrow HNO_3)_{H_2O}} \quad (4)$$

Atmos. Chem. Phys. Discuss., https://doi.org/10.5194/acp-2018-385
Manuscript under review for journal Atmos. Chem. Phys.
Discussion started: 8 May 2018
© Author(s) 2018. CC BY 4.0 License.

Atmospheric Chemistry and Physics Discussions

where $\varepsilon_{O(NO_x \leftrightarrow pNO_3^-)_{OH}}$ and $\varepsilon_{O(NO_x \leftrightarrow pNO_3^-)_{H_2O}}$ represent the O isotope effects associated with pNO_3^- generation through the reaction of NO_x and OH to form HNO_3, and the hydrolysis of N_2O_5 on a wetted surface to form HNO_3, respectively. $\varepsilon_{O(NO_x \leftrightarrow pNO_3^-)_{OH}}$ can be further expressed as:

$$\varepsilon_{O(NO_x \leftrightarrow pNO_3^-)_{OH}} = \varepsilon_{O(NO_x \leftrightarrow HNO_3)_{OH}} = \frac{2}{3}\varepsilon_{O(NO_2 \leftrightarrow HNO_3)_{OH}} + \frac{1}{3}\varepsilon_{O(NO \leftrightarrow HNO_3)_{OH}}$$
$$= \frac{2}{3}\left[\frac{1000\left({}^{18}\alpha_{NO_2/NO} - 1\right)\left(1 - f_{NO_2}\right)}{\left(1 - f_{NO_2}\right) + \left({}^{18}\alpha_{NO_2/NO} \times f_{NO_2}\right)} + \left(\delta^{18}\text{O-NO}_x\right)\right] + \qquad (5)$$
$$\frac{1}{3}\left[\left(\delta^{18}\text{O-H}_2\text{O}\right) + 1000\left({}^{18}\alpha_{OH/H_2O} - 1\right)\right]$$

and $\varepsilon_{O(NO_x \leftrightarrow pNO_3^-)_{H_2O}}$ can be determined as follows:

$$\varepsilon_{O(NO_x \leftrightarrow pNO_3^-)_{H_2O}} = \varepsilon_{O(NO_x \leftrightarrow HNO_3)_{H_2O}} = \frac{5}{6}\left(\delta^{18}\text{O-N}_2\text{O}_5\right) + \frac{1}{6}\left(\delta^{18}\text{O-H}_2\text{O}\right) \qquad (6)$$

where ${}^{18}\alpha_{NO_2/NO}$ and ${}^{18}\alpha_{OH/H_2O}$ represent the equilibrium O isotope fractionation factors between NO_2 and NO, and OH and H_2O, respectively. The range of δ^{18}O-H_2O can be approximated using an estimated tropospheric water vapor δ^{18}O range of -25‰-0‰. The δ^{18}O values for NO_2 and N_2O_5 range from 90‰ to 122‰ (Zong et al. 2017).

${}^{15}\alpha_{NO_2/NO}$ and ${}^{15}\alpha_{N_2O_5/NO_2}$, ${}^{18}\alpha_{NO_2/NO}$ and ${}^{18}\alpha_{OH/H_2O}$ in these equations, are dependent on the temperature, which can be expressed as:

$$1000\left({}^{m}\alpha_{X/Y} - 1\right) = \frac{A}{T^4} \times 10^{10} + \frac{B}{T^3} \times 10^{8} + \frac{C}{T^2} \times 10^{6} + \frac{D}{T} \times 10^{4} \qquad (7)$$

where A, B, C, and D are experimental constants (Table S1) over the temperature range of 150-450 K (Walters and Michalski, 2015; Walters et al., 2016; Walters and Michalski, 2016; Zong et al., 2017).

Based on Equations 4-7 and measured values for δ^{18}O-pNO_3^- of ambient $PM_{2.5}$, a Monte

Atmos. Chem. Phys. Discuss., https://doi.org/10.5194/acp-2018-385
Manuscript under review for journal Atmos. Chem. Phys.
Discussion started: 8 May 2018
© Author(s) 2018. CC BY 4.0 License.

Atmospheric Chemistry and Physics Discussions

Carlo simulation was performed to generate 10000 feasible solutions. The error between predicted and measured $\delta^{18}O$ was less than 0.5‰. The range (maximum and minimum) of computed contribution ratios (γ) were then integrated in Equation 1 to generate an estimate range for the nitrogen isotope effect ε_N (using Equations 2-3). $\delta^{15}N$-pNO_3^- values can be calculated based on ε_N and the estimated $\delta^{15}N$ range for atmospheric NO_x, (see section 2.4).

2.4 Bayesian isotope mixing model

Isotopic mixing models allow estimating the relative contribution of multiple sources (e.g., emission sources of NO_x) within a mixed pool (e.g., ambient pNO_3^-). By explicitly considering the uncertainty associated with the isotopic signatures of any given source, as well as isotope fractionation during the formation of various components of a mixture, the application of Bayesian methods to stable isotope mixing models generates robust probability estimates of source proportions, and are often more appropriate when targeting natural systems than simple linear mixing models (Chang et al., 2016a). Here the Bayesian model MixSIR (a stable isotope mixing model using sampling-importance-resampling) was used to disentangle multiple NO_x sources by generating potential solutions of source apportionment as true probability distributions, which has been widely applied in a number of fields. Details on the model frame and computing methods are given in SI Text S1.

Here, coal combustion (13.72 ± 4.57‰), transportation (-3.71 ± 10.40‰), biomass burning (1.04 ± 4.13‰), and biogenic emissions from soils (-33.77 ± 12.16‰) were considered to be the most relevant contributors of NO_x (Table S2 and Text S2). The $\delta^{15}N$ of atmospheric NO_x is unknown. However, it can be assumed that its range in the atmosphere is constrained by the $\delta^{15}N$ of the NO_x sources and the $\delta^{15}N$ of pNO_3^- after equilibrium fractionation conditions have been reached. Following Zong et al. (2017), $\delta^{15}N$-NO_x in the atmosphere was determined performing iterative model simulations, with a simulation step of 0.01 times the equilibrium fractionation value based on the $\delta^{15}N$-NO_x values of the emission sources (mean and standard deviation) and the

© Author(s) 2018. CC BY 4.0 License.

328 measured δ^{15}N-pNO$_3^-$ of ambient PM$_{2.5}$ (Fig. S2).

329 **3 Results**

330 **3.1 Sanjiang in Northern China**

331 The δ^{15}N-pNO$_3^-$ and δ^{18}O-pNO$_3^-$ values of the eight samples collected from the
332 Sanjiang biomass burning field experiment, ranged from 9.54 to 13.77‰ (mean:
333 12.17‰) and 57.17 to 75.09‰ (mean: 63.57‰), respectively. In this study, atmospheric
334 concentrations of levoglucosan quantified from PM$_{2.5}$ samples collected near the sites
335 of biomass burning in Sanjiang vary between 4.0 and 20.5 μg m^{-3}, two to five orders of
336 magnitude higher than those measured during non-biomass burning season (Cao et al.,
337 2017; Cao et al., 2016). Levoglucosan is an anhydrosugar formed during pyrolysis of
338 cellulose at temperatures above 300 °C (Simoneit, 2002). Due to its specificity for
339 cellulose combustion, it has been widely used as a molecular tracer for biomass burning
340 (Simoneit et al., 1999; Liu et al., 2013a; Jedynska et al., 2014; Liu et al., 2014). Indeed,
341 the concentrations of levoglucosan and aerosol nitrate in Sanjiang were highly
342 correlated (R^2 = 0.64; Fig. 2a), providing compelling evidence that particulate nitrate
343 measured during our study period was predominately derived from biomass burning
344 emissions.

345 **3.2 Nanjing in Eastern China**

346 The mass concentrations $\left(mean_{\min}^{\max} \pm 1\sigma, n = 43\right)$ of PM$_{2.5}$ and pNO$_3^-$ measured in Nanjing
347 City were $122.1_{39.0}^{227.8} \pm 47.9$ and $17.8_{4.0}^{45.2} \pm 10.3$ μg m^{-3}, respectively. All PM$_{2.5}$
348 concentrations exceeded the Chinese Air Quality Standard for daily PM$_{2.5}$ (35 μg m^{-3}),
349 suggesting severe haze pollution during the sampling period. The corresponding δ^{15}N-
350 pNO$_3^-$ values (raw data without correction) ranged between 5.39‰ and 17.99‰,
351 indicating significant enrichment in ^{15}N relative to rural and coastal marine atmospheric
352 NO$_3^-$ sources (Table S4). This may be due to the prominent contribution of fossil fuel-
353 related NO$_x$ emissions with higher δ^{15}N values in urban areas (Elliott et al., 2007; Park

© Author(s) 2018. CC BY 4.0 License.

et al., 2018).

4 Discussion

4.1 Sanjiang campaign: theoretical calculation and field validation of N isotope fractionation during pNO_3^- formation

To be used as a quantitative tracer of biomass-combustion-generated aerosols, levoglucosan must be conserved during its transport from its source, without partial removal by reactions in the atmosphere (Hennigan et al., 2010). The mass concentrations of non-sea-salt potassium (nss-K^+ = K^+ - 0.0355*Na^+) is considered as an independent/additional indicator of biomass burning (Fig. 2b). The association of elevated levels of levoglucosan with high nss-K^+ concentrations underscores that the two compounds derived from the same proximate sources, and that thus aerosol levoglucosan in Sanjiang was indeed pristine and represented a reliable source indicator that is unbiased by altering processes in the atmosphere. Moreover, in our previous work (Cao et al., 2017), we observed that there was a much greater enhancement of atmospheric NO_3^- compared to SO_4^{2-} (a typical coal-related pollutant). This additionally points to biomass burning, and not coal-combustion, as the dominant pNO_3^- source in the study area, making SJ and ideal "quasi single source" environment for calibrating the N isotope effect during pNO_3^- formation.

Figure 2.

Our $\delta^{18}O$-pNO_3^- values are well within the broad range of values in previous reports (Zong et al., 2017; Geng et al., 2017; Walters and Michalski, 2016). However, as depicted in Fig. 3, the $\delta^{15}N$ values of biomass burning-emitted NO_3^- fall within the range of $\delta^{15}N$-NO_x values typically reported for emissions from coal combustion, whereas they are significantly higher than the well-established values for $\delta^{15}N$-NO_x

Atmos. Chem. Phys. Discuss., https://doi.org/10.5194/acp-2018-385
Manuscript under review for journal Atmos. Chem. Phys.
Discussion started: 8 May 2018
© Author(s) 2018. CC BY 4.0 License.

Atmospheric Chemistry and Physics Discussions

emitted from the burning of various types of biomass (mean: 1.04 ± 4.13‰, ranging from -7 to +12‰) (Fibiger and Hastings, 2016). Turekian et al. (1998) conducted laboratory tests involving the burning of eucalyptus and African grasses, and determined that the δ^{15}N of pNO$_3^-$ (around 23‰) was 6.6‰ higher than the δ^{15}N of the burned biomass. This implies significant N isotope partitioning during biomass burning. In the case of complete biomass combustion, by mass balance, the first gaseous products (i.e., NO$_x$) have the same δ^{15}N as the biomass. Hence any discrepancy between the pNO$_3^-$ and the δ^{15}N of the biomass can be attributed to the N isotope fractionation associated with the partial conversion of gaseous NO$_x$ to aerosol NO$_3^-$. Based on the computational quantum chemistry (CQC) module calculations, the N isotope fractionation ε_N $\left(mean_{\min}^{\max} \pm 1\sigma\right)$ determined from the Sanjiang data was $10.99_{10.30}^{12.54} \pm 0.74‰$. After correcting the primary δ^{15}N-pNO$_3^-$ values under the consideration of ε_N, the resulting mean δ^{15}N of $1.17_{-1.89}^{2.98} \pm 1.95‰$ is very close to the N isotopic signature expected for biomass burning-emitted NO$_x$ (1.04 ± 4.13‰) (Fig. 3) (Fibiger and Hastings, 2016). The much higher δ^{15}N-pNO$_3^-$ values in our study compared to reported δ^{15}N-NO$_x$ values for biomass burning can easily be reconciled when including N isotope fractionation during the conversion of NO$_x$ to NO$_3^-$. Put another way, given that Sanjiang is an environment where we can essentially exclude NO$_x$ sources other than biomass burning at the time of sampling, the data nicely validate our CQC module-based approach to estimate ε_N.

Figure 3.

4.2 Source apportionment of NO$_x$ in an urban setting using a Bayesian isotopic mixing model

Due to its high population density and intensive industrial production, the Nanjing

Atmos. Chem. Phys. Discuss., https://doi.org/10.5194/acp-2018-385
Manuscript under review for journal Atmos. Chem. Phys.
Discussion started: 8 May 2018
© Author(s) 2018. CC BY 4.0 License.

Atmospheric Chemistry and Physics Discussions

atmosphere was expected to have high NO_x concentrations derived from road traffic and coal combustion (Zhao et al., 2015). However, the raw δ^{15}N-$p$$NO_3^-$ values (10.93 ± 3.32‰) fell well within the variation range of coal-emitted δ^{15}N-NO_x (Fig. 3). It is tempting to conclude that coal combustion is the main, or even sole, $p$$NO_3^-$ source (given the equivalent δ^{15}N values), yet, this is very unlikely. The data rather confirm that significant isotope fractionation occurred during the conversion of NO_x to NO_3^- and that, without consideration of the N isotope effect, traffic-related NO_x emissions will be markedly underestimated.

In the atmosphere, the oxygen atoms of NO_x rapidly exchanged with O_3 in the NO/NO_2 cycle (see equations R_1-R_3) (Hastings et al., 2003), and the δ^{18}O-$p$$NO_3^-$ values are determined by its production pathways (R_4-R_7), rather than the sources of NO_x (Hastings et al., 2003). Thus, δ^{18}O-$p$$NO_3^-$ can be used to gain information on the pathway of conversion of NO_x to nitrate in the atmosphere (Fang et al., 2011). In the computational quantum chemistry module used here to calculate isotope fractionation, we assumed that two-thirds of the oxygen atoms in NO_3^- derive from O_3 and one-third from •OH in the •OH generation pathway (R_4) (Hastings et al., 2003); correspondingly, five sixths of the oxygen atoms then derived from O_3 and one sixth from •OH in the O_3/H_2O pathway (R_5-R_7). The assumed range for δ^{18}O-O_3 and δ^{18}O-H_2O values were 90‰-122‰ and -25‰-0‰, respectively (Zong et al., 2017). The partitioning between the two possible pathways was then assessed through Monte Carlo simulation (Zong et al., 2017). The estimated range was rather broad, given the wide range of δ^{18}O-O_3 and δ^{18}O-H_2O values used. Nevertheless, the theoretical calculation of the average contribution ratio (γ) for nitrate formation in Nanjing via the reaction of NO_2 and •OH is consistent with the results from simulations using the Weather Research and Forecasting model coupled with Chemistry (WRF-Chem) (Fig. 4; see Text S3 for details). A clear diurnal cycle of the mass concentration of nitrate formed through •OH oxidation of NO_2 can be observed (Fig. S3), with much higher concentrations between 12:00 and 18:00, This indicates the importance of photochemically produced •OH during daytime. Yet, throughout our sampling period in Nanjing, the average $p$$NO_3^-$

© Author(s) 2018. CC BY 4.0 License.

435 formation by the heterogeneous hydrolysis of N_2O_5 (12.6 μg m^{-3}) exceeded pNO_3^-
436 formation by the reaction of NO_2 and •OH (4.8 μg m^{-3}), even during daytime, consistent
437 with recent observations during peak pollution periods in Beijing (Wang et al., 2017).
438 Given that the production rates of N_2O_5 in the atmosphere is governed by ambient O_3
439 concentrations, reducing atmospheric O_3 levels appears to be one of the utmost
440 important measures to take for mitigating pNO_3^- pollution in China's urban
441 atmospheres.

442

443 **Figure 4**.

444

445 In Nanjing, dependent on the time-dependent, dominant pNO_3^- formation pathway, the
446 average N isotope fractionation value calculated using the computational quantum
447 chemistry module varied between 10.77‰ and 19.34‰ (15.33‰ on average). Using
448 the Bayesian model MixSIR, the contribution of each source can be estimated, based
449 on the mixed-source isotope data under the consideration of prior information on the
450 site (see Text S1 for detailed information regarding model frame and computing
451 method). As described above, theoretically, there are four major sources, i.e., road
452 traffic, coal combustion, biomass burning, and biogenic soil, potentially contributing to
453 ambient NO_x. As a start, we tentatively integrated all four sources into MixSIR (data
454 not shown). The relative contribution of biomass burning to the ambient NO_x (median
455 value) ranged from 28% to 70% (average 42%), representing the most important source.
456 The primary reason for such apparently high contribution by biomass burning is that
457 the corrected $\delta^{15}N$-pNO_3^- values of $-4.29^{0.42}_{-10.32} \pm 3.66$‰ are relatively close to the N
458 isotopic signature of biomass burning-emitted NO_x (1.04 ± 4.13‰) compared to the
459 other possible sources. Based on $\delta^{15}N$ alone, the isotope approach can be ambiguous if
460 there are more than two sources. The N isotope signature of NO_x from biomass burning
461 falls right in between the spectrum of plausible values, with highest $\delta^{15}N$ for emissions
462 from coal combustion on the one end, and much lower values for automotive and soil

© Author(s) 2018. CC BY 4.0 License.

463 emissions on the other, and will be similar to a mixed signature from coal combustion
464 and NO_x emissions from traffic.

465 We can make several evidence-based pre-assumption to better constrain the emission
466 sources in the mixing model analysis: (1) sampling at a typical urban site in a major
467 industrial city in China, we can assume that the sources of road traffic and coal
468 combustion are dominant, while the contribution of biogenic soil to ambient NO_x
469 should have minimal impact, or can be largely neglected (Zhao et al., 2015); (2) there
470 is no crop harvest activity in Eastern China during the winter season. Furthermore,
471 deforestation and combustion of fuelwood has been discontinued in China's major
472 cities (Chang et al., 2016a). Therefore, the contribution of biomass burning-emitted
473 NO_x during the sampling period should also be minor. Indeed, Fig. S4 shows that the
474 mass concentration of biomass burning-related pNO_3^- is not correlated with the fraction
475 of levoglucosan that contributes to OC, confirming a weak impact of biomass burning
476 on the variation of pNO_3^- concentration during our study period.

477 In a second, alternative, and more realistic scenario, we excluded biomass burning and
478 soil as potential source of NO_x in MixSIR (see above). As illustrated in Fig. 5a,
479 assuming that NO_x emissions in urban Nanjing during our study period originated
480 solely from road traffic and coal combustion, their relative contribution to the mass
481 concentration of pNO_3^- is 12.5 ± 9.1 μg m^{-3} (or 68 ± 11%) and 4.9 ± 2.5 μg m^{-3} (or 32
482 ± 11%), respectively. These numbers agree well with a city-scale NO_x emission
483 inventory established for Nanjing recently (Zhao et al., 2015). Nevertheless, on a
484 nation-wide level, relatively large uncertainties with regards to the overall fossil fuel
485 consumption and fuel types propagate into large uncertainties of NO_x concentration
486 estimates and predictions of longer-term emission trends (Li et al., 2017). Current
487 emission-inventory estimates (Jaegle et al., 2005; Zhang et al., 2012; Liu et al., 2015;
488 Zhao et al., 2013) suggest that in 2010 NO_x emissions from coal-fired power plants in
489 China were about 30% higher than those from transportation. However, our isotope-
490 based source apportionment of NO_x clearly shows that in 2014 the contribution from
491 road traffic to NO_x emissions, at least in Nanjing (a city that can be considered

© Author(s) 2018. CC BY 4.0 License.

492 representative for most densely populated areas in China) is twice that of coal
493 combustion. In fact, due to changing economic activities, emission sources of air
494 pollutants in China are changing rapidly. For example, over the past several years,
495 China has implemented an extended portfolio of plans to phase out its old-fashioned
496 and small power plants, and to raise the standards for reducing industrial pollutant
497 emissions (Chang, 2012). On the other hand, China continuously experienced double-
498 digit annual growth in terms of auto sales during the 2000s, and in 2009 it became the
499 world's largest automobile market (Liu et al., 2013b; Chang et al., 2017; Chang et al.,
500 2016b). Recent satellite-based studies successfully analyzed the NO_x vertical column
501 concentration ratios for megacities in Eastern China and highlighted the importance of
502 transportation-related NOx emissions (Reuter et al., 2014; Gu et al., 2014; Duncan et
503 al., 2016; Jin et al., 2017). Moreover, long-term measurements of the ratio of NO_3^-
504 versus non-sea-salt SO_4^{2-} in precipitation and aerosol jointly revealed a continuously
505 increasing trend in Eastern China throughout the latest decade, suggesting decreasing
506 emissions from coal combustion (Liu et al., 2013b; Itahashi et al., 2017). Both coal
507 combustion- and road traffic-related pNO_3^- concentrations are highly correlated with
508 their corresponding tracers (i.e., SO_2 and CO, respectively), confirming the validity of
509 our MixSIR modelling results. With justified confidence in our Bayesian isotopic model
510 results, we conclude that previous estimates of NO_x emissions from
511 automotive/transportation sources in China based on bottom-up emission inventories
512 may be too low.

513

514 **Figure 5**.

515

516 **3.3 Previous $\delta^{15}N$-NO_3^- based estimates on NO_x sources**

517 Stable nitrogen isotope ratios of nitrate have been used to identify nitrogen sources in
518 various environments in China, often without large differences in $\delta^{15}N$ between

© Author(s) 2018. CC BY 4.0 License.

519 rainwater and aerosol NO_3^- (Kojima et al., 2011). In previous work, no consideration
520 was given to potential N isotope fractionation during atmospheric pNO_3^- formation.
521 Here, we reevaluated 700 data points of δ^{15}N-NO_3^- in aerosol (-0.77 ± 4.52‰, n = 308)
522 and rainwater (3.79 ± 6.14‰, n = 392) from 13 sites that are located in the area of
523 mainland China and the Yellow and East and South China Seas (Fig. 1), extracted from
524 the literature (see SI Table S4 for details). To verify the potentially biasing effects of
525 neglecting N isotope fractionation (i.e. testing the sensitivity of ambient NO_x source
526 contribution estimates to the effect of N isotope fractionation), the Bayesian isotopic
527 mixing model was applied a) to the original NO_3^- isotope data set and b) to the corrected
528 nitrate isotope data set, accounting for the N isotope fractionation during NO_x
529 transformation. All 13 sampling sites are located in non-urban areas; therefore, apart
530 from coal combustion and on-road traffic, the contributions of biomass burning and
531 biogenic soil to nitrate needs to be taken into account.

532 Although most of the sites are located in rural and coastal environments, using the
533 original data set without the consideration of N isotope fractionation in the Bayesian
534 isotopic mixing model, fossil fuel-related NO_x emissions (coal combustion and on-road
535 traffic) appear as the largest contributor at all the sites (data are not shown). This is
536 particularly true for coal combustion: Everywhere, except for the sites of Dongshan
537 Islands and Mt. Lumin, NO_x emissions seem to be dominated by coal combustion. Very
538 high contribution from coal combustion (on the order of 40-60%) particularly in
539 Northern China may be plausible, and can be attributed to a much larger consumption
540 of coal. Yet, rather unlikely, the highest estimated contribution of coal combustion (83%)
541 was calculated for Beihuang Island (a full-year sampling at a costal island that is 65 km
542 north of Shandong Peninsula and 185 km east of the Beijing-Tianjin-Hebei region) and
543 not for mainland China. While Beihuang may be an extreme example, we argue that,
544 collectively, the contribution of coal combustion to ambient NO_x in China as calculated
545 on the basis of isotopic analyses in previous studies without the consideration of N
546 isotope fractionation represent overestimates.

547 As a first step towards a more realistic assessment of the actual partitioning of NO_x

© Author(s) 2018. CC BY 4.0 License.

548 sources in China in general (and coal combustion-emitted NO_x in particular), it is
549 imperative to determine the location-specific values for ε_N. Unfortunately, without
550 $\delta^{18}O\text{-}NO_3^-$ data in hand, as well as data on meteorological parameters that correspond
551 to the 700 $\delta^{15}N\text{-}NO_3^-$ values used in our meta-analysis, it is not possible to estimate the
552 ε_N values through the above-mentioned CQC module. As a viable alternative, we
553 adopted the approximate values for ε_N as estimated in Sanjiang (10.99‰) and Nanjing
554 (15.33 ± 4.90‰). As indicated in Fig. 6, the estimates on the source partitioning is
555 sensitive to the choice of ε_N. Whereas with increasing ε_N, estimates on the relative
556 contribution of on-road traffic and biomass burning remained relatively stable;
557 estimates for coal combustion and biogenic soil changed significantly, in opposite
558 directions. More precisely, depending on ε_N, the average estimate of the fractional
559 contribution of coal combustion decreased drastically from 43% (ε_N = 0‰) to 5% (ε_N
560 = 20‰) (Fig. 6), while the contribution from biogenic soil to NO_x emissions increased
561 in a complementary way. Given the lack of better constraints on ε_N for the 13 sampling
562 sites, it cannot be our goal here to provide a robust revised estimate on the partitioning
563 of NO_x sources throughout China and its neighboring areas. But we have very good
564 reasons to assume that disregard of N isotope fractionation during pNO_3^- formation in
565 previous isotope-based source apportionment studies has likely led to overestimates of
566 the relative contribution of coal combustion to total NO_x emissions in China. For what
567 we would consider the most conservative estimate, i.e. lowest calculated value for the
568 N isotope fractionation during the transformation of NO_x to pNO_3^- (ε_N = 5‰), the
569 approximate contribution from coal combustion to the NO_x pool would be 28%, more
570 than 30% less than N isotope mixing model-based estimates would yield without
571 consideration of the N isotope fractionation (i.e., εN = 0‰) (Fig. 6).

572

573 **Figure 6.**

574

© Author(s) 2018. CC BY 4.0 License.

575

576 4 Conclusion and outlook

577 Consistent with theoretical predictions, δ^{15}N-pNO$_3^-$ data from a field experiment where
578 atmospheric pNO$_3^-$ formation could be attributed reliably to NO$_x$ from biomass burning
579 only, revealed that the conversion of NO$_x$ to pNO$_3^-$ is associated with a significant net
580 N isotope effect (ε_N). It is imperative that future studies, making use of isotope mixing
581 models to gain conclusive constraints on the source partitioning of atmospheric NO$_x$,
582 will consider this N isotope fractionation. The latter will change with time and space,
583 depending on the distribution of ozone and OH radicals in the atmosphere and the
584 predominant NO$_x$ chemistry. The O-isotope signatures of pNO$_3^-$ is mostly chemistry-
585 (and not source) driven (modulated by O-isotope exchange reactions in the atmosphere),
586 and thus, O isotope measurements do not allow addressing the ambiguities with regards
587 to the NO$_x$ source that may remain when just looking at δ^{15}N values alone. However,
588 δ^{18}O in pNO$_3^-$ will help assessing the relative importance of the dominant pNO$_3^-$
589 formation pathway. Simultaneous δ^{15}N and δ^{18}O measurements of atmospheric nitrate
590 thus allow reliable information on ε_N, and in turn on the relative importance of single
591 NO$_x$ sources. For example, for Nanjing, which can be considered representative for
592 other large cities in China, dual-isotopic and chemical-tracer evidence suggest that on-
593 road traffic and coal-fired power plants, rather than biomass burning, are the
594 predominant sources during high-haze pollution periods. Given that the increasing
595 frequency of nitrate-driven haze episodes in China, our findings are critically important
596 in terms of guiding the use of stable nitrate isotope measurements to evaluate the
597 relative importance of single NO$_x$ sources on regional scales, and for adapting suitable
598 mitigation measures. Future assessments of NO$_x$ emissions in China (and elsewhere)
599 should involve simultaneous δ^{15}N and δ^{18}O measurements of atmospheric nitrate and
600 NO$_x$ at high spatiotemporal resolution, allowing us to more quantitatively reevaluate
601 former N-isotope based NO$_x$ source partitioning estimates.

602 Competing interests

© Author(s) 2018. CC BY 4.0 License.

603 The authors declare that they have no competing interests.

604 **Data availability**

605 Data are available from the corresponding author on request.

606 **Acknowledgements**

607 This study was supported by the National Key Research and Development Program of
608 China (2017YFC0210101), the National Natural Science Foundation of China (Grant
609 nos. 91644103, 41705100, and 41575129), the Provincial Natural Science Foundation
610 of Jiangsu (BK20170946), the University Science Research Project of Jiangsu Province
611 (17KJB170011), and through University Basel Research funds.

612

613 **Reference**

614 Altieri, K. E., Hastings, M. G., Gobel, A. R., Peters, A. J., and Sigman, D. M.: Isotopic
615 composition of rainwater nitrate at Bermuda: the influence of air mass source and
616 chemistry in the marine boundary layer, J. Geophys. Res., 118, 11, 304-311, 316,
617 doi: 10.1002/jgrd.50829, 2013.
618 Anenberg, S. C., Miller, J., Minjares, R., Du, L., Henze, D. K., Lacey, F., Malley, C. S.,
619 Emberson, L., Franco, V., Klimont, Z., and Heyes, C.: Impacts and mitigation of
620 excess diesel-related NO_x emissions in 11 major vehicle markets, Nature, 545, 467-
621 471, doi: 10.1038/nature22086, 2017.
622 Böhlke, J. K., Mroczkowski, S. J., and Coplen, T. B.: Oxygen isotopes in nitrate: new
623 reference materials for ^{18}O:^{17}O:^{16}O measurements and observations on nitrate-water
624 equilibration, Rapid Commun. Mass Sp., 17, 1835-1846, doi: 10.1002/rcm.1123,
625 2003.
626 Cao, F., Zhang, S. C., Kawamura, K., and Zhang, Y. L.: Inorganic markers,
627 carbonaceous components and stable carbon isotope from biomass burning aerosols
628 in Northeast China, Sci. Total Environ., 572, 1244-1251, doi:
629 10.1016/j.scitotenv.2015.09.099, 2016.
630 Cao, F., Zhang, S. C., Kawamura, K., Liu, X., Yang, C., Xu, Z., Fan, M., Zhang, W.,
631 Bao, M., Chang, Y., Song, W., Liu, S., Lee, X., Li, J., Zhang, G., and Zhang, Y. L.:
632 Chemical characteristics of dicarboxylic acids and related organic compounds in
633 $PM_{2.5}$ during biomass-burning and non-biomass-burning seasons at a rural site of
634 Northeast China, Environ. Pollut., 231, 654-662, doi: 10.1016/j.envpol.2017.08.045,
635 2017.
636 Casciotti, K. L., Sigman, D. M., Hastings, M. G., Böhlke, J. K., and Hilkert, A.:
637 Measurement of the oxygen isotopic composition of nitrate in seawater and
638 freshwater using the denitrifier method, Anal. Chem., 74, 4905-4912, doi:

© Author(s) 2018. CC BY 4.0 License.

639 10.1021/ac020113w, 2002.
640 Chang, Y.: China needs a tighter $PM_{2.5}$ limit and a change in priorities, Environ. Sci.
641 Technol., 46, 7069-7070, doi: 10.1021/es3022705, 2012.
642 Chang, Y., Liu, X., Deng, C., Dore, A. J., and Zhuang, G.: Source apportionment of
643 atmospheric ammonia before, during, and after the 2014 APEC summit in Beijing
644 using stable nitrogen isotope signatures, Atmos. Chem. Phys., 16, 11635-11647, doi:
645 10.5194/acp-16-11635-2016, 2016a.
646 Chang, Y., Zou, Z., Deng, C., Huang, K., Collett, J. L., Lin, J., and Zhuang, G.: The
647 importance of vehicle emissions as a source of atmospheric ammonia in the megacity
648 of Shanghai, Atmos. Chem. Phys., 16, 3577-3594, doi: 10.5194/acp-16-3577-2016,
649 2016b.
650 Chang, Y., Deng, C., Cao, F., Cao, C., Zou, Z., Liu, S., Lee, X., Li, J., Zhang, G., and
651 Zhang, Y.: Assessment of carbonaceous aerosols in Shanghai, China - Part 1: long-
652 term evolution, seasonal variations, and meteorological effects, Atmos. Chem. Phys.,
653 17, 9945-9964, doi: 10.5194/acp-17-9945-2017, 2017.
654 Duncan, B. N., Lamsal, L. N., Thompson, A. M., Yoshida, Y., Lu, Z., Streets, D. G.,
655 Hurwitz, M. M., and Pickering, K. E.: A space-based, high-resolution view of notable
656 changes in urban NO_x pollution around the world (2005-2014), J. Geophys. Res., 121,
657 976-996, doi: 10.1002/2015JD024121, 2016.
658 Elliott, E., Kendall, C., Wankel, S. D., Burns, D., Boyer, E., Harlin, K., Bain, D., and
659 Butler, T.: Nitrogen isotopes as indicators of NO_x source contributions to atmospheric
660 nitrate deposition across the midwestern and northeastern United States, Environ. Sci.
661 Technol., 41, 7661-7667, doi: 10.1021/es070898t, 2007.
662 Elliott, E. M., Kendall, C., Boyer, E. W., Burns, D. A., Lear, G. G., Golden, H. E., Harlin,
663 K., Bytnerowicz, A., Butler, T. J., and Glatz, R.: Dual nitrate isotopes in dry
664 deposition: Utility for partitioning NO_x source contributions to landscape nitrogen
665 deposition, J. Geophys. Res., 114, doi: 10.1029/2008jg000889, 2009.
666 Fang, Y. T., Koba, K., Wang, X. M., Wen, D. Z., Li, J., Takebayashi, Y., Liu, X. Y., and
667 Yoh, M.: Anthropogenic imprints on nitrogen and oxygen isotopic composition of
668 precipitation nitrate in a nitrogen-polluted city in southern China, Atmos. Chem.
669 Phys., 11, 1313-1325, doi: 10.5194/acp-11-1313-2011, 2011.
670 Felix, J. D., Elliott, E. M., and Shaw, S. L.: Nitrogen isotopic composition of coal-fired
671 power plant NO_x: Influence of emission controls and implications for global emission
672 inventories, Environ. Sci. Technol., 46, 3528-3535, doi: 10.1021/es203355v, 2012.
673 Felix, J. D., Elliott, E. M., Gish, T. J., McConnell, L. L., and Shaw, S. L.: Characterizing
674 the isotopic composition of atmospheric ammonia emission sources using passive
675 samplers and a combined oxidation-bacterial denitrifier approach, Rapid Comm.
676 Mass spec., 27, 2239-2246, doi: 10.1002/rcm.6679, 2013.
677 Felix, J. D., and Elliott, E. M.: Isotopic composition of passively collected nitrogen
678 dioxide emissions: Vehicle, soil and livestock source signatures, Atmos. Environ., 92,
679 359-366, doi: 10.1016/j.atmosenv.2014.04.005, 2014.
680 Fibiger, D. L., and Hastings, M. G.: First measurements of the nitrogen isotopic
681 composition of NO_x from biomass burning, Environ. Sci. Technol., 50, 11569-11574,
682 doi: 10.1021/acs.est.6b03510, 2016.

© Author(s) 2018. CC BY 4.0 License.

683 Freyer, H.: Seasonal trends of NH_4^+ and NO_3^- nitrogen isotope composition in rain
684 collected at Jülich, Germany, Tellus, 30, 83-92, 1978.
685 Freyer, H. D., Kley, D., Volz-Thomas, A., and Kobel, K.: On the interaction of isotopic
686 exchange processes with photochemical reactions in atmospheric oxides of nitrogen,
687 J. Geophys. Res., 98, 14791-14796, doi: 10.1029/93JD00874, 1993.
688 Freyer, H. D.: Seasonal variation of $^{15}N/^{14}N$ ratios in atmospheric nitrate species, Tellus,
689 43, 30-44, doi: 10.3402/tellusb.v43i1.15244, 2017.
690 Fu, X., Wang, S., Zhao, B., Xing, J., Cheng, Z., Liu, H., and Hao, J.: Emission inventory
691 of primary pollutants and chemical speciation in 2010 for the Yangtze River Delta
692 region, China, Atmos. Environ., 70, 39-50, doi: 10.1016/j.atmosenv.2012.12.034,
693 2013.
694 Galloway, J. N., Aber, J. D., Erisman, J. W., Seitzinger, S. P., Howarth, R. W., Cowling,
695 E. B., and Cosby, B. J.: The nitrogen cascade, Biosci., 53, 341-356, doi:
696 10.1641/0006-3568(2003)053[0341:Tnc]2.0.Co;2, 2003.
697 Geng, L., Murray, L. T., Mickley, L. J., Lin, P., Fu, Q., Schauer, A. J., and Alexander,
698 B.: Isotopic evidence of multiple controls on atmospheric oxidants over climate
699 transitions, Nature, 546, 133-136, doi: 10.1038/nature22340, 2017.
700 Gobel, A. R., Altieri, K. E., Peters, A. J., Hastings, M. G., and Sigman, D. M.: Insights
701 into anthropogenic nitrogen deposition to the North Atlantic investigated using the
702 isotopic composition of aerosol and rainwater nitrate, Geophys. Res. Lett., 40, 5977-
703 5982, doi: 10.1002/2013GL058167, 2013.
704 Gu, D., Wang, Y., Smeltzer, C., and Boersma, K. F.: Anthropogenic emissions of NO_x
705 over China: Reconciling the difference of inverse modeling results using GOME-2
706 and OMI measurements, J. Geophys. Res., 119, 7732-7740, doi:
707 10.1002/2014JD021644, 2014.
708 Hastings, M. G., Sigman, D. M., and Lipschultz, F.: Isotopic evidence for source
709 changes of nitrate in rain at Bermuda, J. Geophys. Res., 108, doi:
710 10.1029/2003JD003789, 2003.
711 Heaton, T. H. E.: $^{15}N/^{14}N$ ratios of NO_x from vehicle engines and coal-fired power
712 stations, Tellus, 42, 304-307, doi: 10.1034/j.1600-0889.1990.00007.x-i1, 1990.
713 Hennigan, C. J., Sullivan, A. P., Collett, J. L., and Robinson, A. L.: Levoglucosan
714 stability in biomass burning particles exposed to hydroxyl radicals, Geophys. Res.
715 Lett., 37, doi: 10.1029/2010GL043088, 2010.
716 Hoering, T.: The isotopic composition of the ammonia and the nitrate ion in rain,
717 Geochim. Cosmochim. Ac., 12, 97-102, doi: 10.1016/0016-7037(57)90021-2, 1957.
718 Itahashi, S., Yumimoto, K., Uno, I., Hayami, H., Fujita, S. I., Pan, Y., and Wang, Y.: A
719 15-year record (2001-2015) of the ratio of nitrate to non-seasalt sulfate in
720 precipitation over East Asia, Atmos. Chem. Phys. Discuss., 2017, 1-30, doi:
721 10.5194/acp-2017-848, 2017.
722 Jaegle, L., Steinberger, L., Martin, R. V., and Chance, K.: Global partitioning of NO_x
723 sources using satellite observations: Relative roles of fossil fuel combustion, biomass
724 burning and soil emissions, Faraday Discus., 130, 407-423, doi: 10.1039/B502128F,
725 2005.
726 Jedynska, A., Hoek, G., Wang, M., Eeftens, M., Cyrys, J., Beelen, R., Cirach, M., De

© Author(s) 2018. CC BY 4.0 License.

Nazelle, A., Nystad, W., Makarem Akhlaghi, H., Meliefste, K., Nieuwenhuijsen, M., de Hoogh, K., Brunekreef, B., and Kooter, I. M.: Spatial variations and development of land use regression models of levoglucosan in four European study areas, Atmos. Chem. Phys. Discuss., 2014, 13491-13527, doi: 10.5194/acpd-14-13491-2014, 2014.

Ji, S., Cherry, C. R., Zhou, W., Sawhney, R., Wu, Y., Cai, S., Wang, S., and Marshall, J. D.: Environmental justice aspects of exposure to $PM_{2.5}$ emissions from electric vehicle use in China, Environ. Sci. Technol., 49, 13912-13920, doi: 10.1021/acs.est.5b04927, 2015.

Jin, X., Fiore, A. M., Murray, L. T., Valin, L. C., Lamsal, L. N., Duncan, B., Folkert Boersma, K., De Smedt, I., Abad, G. G., Chance, K., and Tonnesen, G. S.: Evaluating a space-based indicator of surface ozone-NO_x-VOC sensitivity over midlatitude source regions and application to decadal trends, J. Geophys. Res., 122, 439-461, doi: 10.1002/2017JD026720, 2017.

Kendall, C., Elliott, E. M., and Wankel, S. D.: Stable isotopes in ecology and environmental science, chapter 12, 2nd Edition, Blackwell, Oxford, 2007.

Kojima, K., Murakami, M., Yoshimizu, C., Tayasu, I., Nagata, T., and Furumai, H.: Evaluation of surface runoff and road dust as sources of nitrogen using nitrate isotopic composition, Chemosphere, 84, 1716-1722, doi: 10.1016/j.chemosphere.2011.04.071, 2011.

Lamsal, L. N., Martin, R. V., Padmanabhan, A., van Donkelaar, A., Zhang, Q., Sioris, C. E., Chance, K., Kurosu, T. P., and Newchurch, M. J.: Application of satellite observations for timely updates to global anthropogenic NO_x emission inventories, Geophy. Res. Lett., 38, doi: 10.1029/2010GL046476, 2011.

Leighton, P.: Photochemistry of Air Pollution, Academic, New York, 1961.

Levy, H., Moxim, W. J., and Kasibhatla, P. S.: A global three-dimensional time-dependent lightning source of tropospheric NO_x, J. Geophys. Res., 101, 22911-22922, doi: 10.1029/96JD02341, 1996.

Li, D., and Wang, X.: Nitrogen isotopic signature of soil-released nitric oxide (NO) after fertilizer application, Atmos. Environ., 42, 4747-4754, doi: 10.1016/j.atmosenv.2008.01.042, 2008.

Li, M., Zhang, Q., Kurokawa, J. I., Woo, J. H., He, K., Lu, Z., Ohara, T., Song, Y., Streets, D. G., Carmichael, G. R., Cheng, Y., Hong, C., Huo, H., Jiang, X., Kang, S., Liu, F., Su, H., and Zheng, B.: MIX: a mosaic Asian anthropogenic emission inventory under the international collaboration framework of the MICS-Asia and HTAP, Atmos. Chem. Phys., 17, 935-963, doi: 10.5194/acp-17-935-2017, 2017.

Ling, T. Y., and Chan, C. K.: Formation and transformation of metastable double salts from the crystallization of mixed ammonium nitrate and ammonium sulfate particles, Environ. Sci. Technol., 41, 8077-8083, doi: 10.1021/es071419t, 2007.

Liu, D., Li, J., Zhang, Y., Xu, Y., Liu, X., Ding, P., Shen, C., Chen, Y., Tian, C., and Zhang, G.: The use of levoglucosan and radiocarbon for source apportionment of $PM_{2.5}$ carbonaceous aerosols at a background site in East China, Environ. Sci. Technol., 47, 10454-10461, doi: 10.1021/es401250k, 2013a.

Liu, F., Zhang, Q., Tong, D., Zheng, B., Li, M., Huo, H., and He, K. B.: High-resolution inventory of technologies, activities, and emissions of coal-fired power plants in

© Author(s) 2018. CC BY 4.0 License.

China from 1990 to 2010, Atmos. Chem. Phys., 15, 13299-13317, doi: 10.5194/acp-15-13299-2015, 2015.

Liu, J., Li, J., Zhang, Y., Liu, D., Ding, P., Shen, C., Shen, K., He, Q., Ding, X., Wang, X., Chen, D., Szidat, S., and Zhang, G.: Source apportionment using radiocarbon and organic tracers for $PM_{2.5}$ carbonaceous aerosols in Guangzhou, South China: contrasting local- and regional-scale haze events, Environ. Sci. Technol., 48, 12002-12011, doi: 10.1021/es503102w, 2014.

Liu, X., Zhang, Y., Han, W., Tang, A., Shen, J., Cui, Z., Vitousek, P., Erisman, J. W., Goulding, K., Christie, P., Fangmeier, A., and Zhang, F.: Enhanced nitrogen deposition over China, Nature, 494, 459-463, doi: 10.1038/nature11917, 2013b.

Lu, Z., Streets, D. G., de Foy, B., Lamsal, L. N., Duncan, B. N., and Xing, J.: Emissions of nitrogen oxides from US urban areas: estimation from Ozone Monitoring Instrument retrievals for 2005-2014, Atmos. Chem. Phys., 15, 10367-10383, doi: 10.5194/acp-15-10367-2015, 2015.

Michalski, G., Scott, Z., Kabiling, M., and Thiemens, M. H.: First measurements and modeling of $\Delta^{17}O$ in atmospheric nitrate, Geophys. Res. Lett., 30, 1870-1872, doi: 10.1029/2003gl017015, 2003.

Miyazaki, K., Eskes, H., Sudo, K., Boersma, K. F., Bowman, K., and Kanaya, Y.: Decadal changes in global surface NO_x emissions from multi-constituent satellite data assimilation, Atmos. Chem. Phys., 17, 807-837, doi: 10.5194/acp-17-807-2017, 2017.

Morin, S., Savarino, J., Frey, M. M., Yan, N., Bekki, S., Bottenheim, J. W., and Martins, J. M.: Tracing the origin and fate of NO_x in the Arctic atmosphere using stable isotopes in nitrate, Science, 322, 730-732, doi: 10.1126/science.1161910, 2008.

Morino, Y., Kondo, Y., Takegawa, N., Miyazaki, Y., Kita, K., Komazaki, Y., Fukuda, M., Miyakawa, T., Moteki, N., and Worsnop, D. R.: Partitioning of HNO_3 and particulate nitrate over Tokyo: Effect of vertical mixing, J. Geophys. Res., 111, doi: 10.1029/2005JD006887, 2006.

Park, Y. M., Park, K. S., Kim, H., Yu, S. M., Noh, S., Kim, M. S., Kim, J. Y., Ahn, J. Y., Lee, M. D., Seok, K. S., and Kim, Y. H.: Characterizing isotopic compositions of TC-C, NO_3^--N, and NH_4^+-N in $PM_{2.5}$ in South Korea: Impact of China's winter heating, Environ. Pollut., 233, 735-744, doi: 10.1016/j.envpol.2017.10.072, 2018.

Price, C., Penner, J., and Prather, M.: NO_x from lightning: 1. Global distribution based on lightning physics, J. Geophys. Res., 102, 5929-5941, doi: 10.1029/96JD03504, 1997.

Reuter, M., Buchwitz, M., Hilboll, A., Richter, A., Schneising, O., Hilker, M., Heymann, J., Bovensmann, H., and Burrows, J. P.: Decreasing emissions of NOx relative to CO_2 in East Asia inferred from satellite observations, Nat. Geosci., 7, 792-795, doi: 10.1038/ngeo2257, 2014.

Richter, A., Burrows, J. P., Nüß, H., Granier, C., and Niemeier, U.: Increase in tropospheric nitrogen dioxide over China observed from space, Nature, 437, 129, doi: 10.1038/nature04092, 2005.

Savarino, J., Kaiser, J., Morin, S., Sigman, D., and Thiemens, M.: Nitrogen and oxygen isotopic constraints on the origin of atmospheric nitrate in coastal Antarctica, Atmos.

© Author(s) 2018. CC BY 4.0 License.

Chem. Phys., 7, 1925-1945, doi: 10.5194/acp-7-1925-2007, 2007.

Seinfeld, J. H., and Pandis, S. N.: Atmospheric chemistry and physics: From air pollution to climate change, John Wiley & Sons, 2012.

Sigman, D. M., Casciotti, K. L., Andreani, M., Barford, C., Galanter, M., and Böhlke, J. K.: A bacterial method for the nitrogen isotopic analysis of nitrate in seawater and freshwater, Anal. Chem., 73, 4145-4153, doi: 10.1021/ac010088e, 2001.

Simoneit, B. R. T., Schauer, J. J., Nolte, C. G., Oros, D. R., Elias, V. O., Fraser, M. P., Rogge, W. F., and Cass, G. R.: Levoglucosan, a tracer for cellulose in biomass burning and atmospheric particles, Atmos. Environ., 33, 173-182, Anal. Chem., doi: 10.1016/S1352-2310(98)00145-9, 1999.

Simoneit, B. R. T.: Biomass burning - a review of organic tracers for smoke from incomplete combustion, Appl. Geochem., 17, 129-162, Anal. Chem., doi: 10.1016/S0883-2927(01)00061-0, 2002.

Smith, M. L., Bertram, A. K., and Martin, S. T.: Deliquescence, efflorescence, and phase miscibility of mixed particles of ammonium sulfate and isoprene-derived secondary organic material, Atmos. Chem. Phys., 12, 9613-9628, doi: 10.5194/acp-12-9613-2012, 2012.

Solomon, S., Qin, D., Manning, M., Chen, Z., Marquis, M., Averyt, K. B., Tignor, M., and Miller, H. L.: Climate change 2007: The physical science basis: contribution of Working Group I to the Fourth Assessment Report of the Intergovernmental Panel on Climate Change, Cambridge University Press, New York, 2007.

Thiemens, M. H., and Heidenreich, J. E.: The mass-independent fractionation of oxygen: a novel isotope effect and its possible cosmochemical implications, Science, 219, 1073-1075, doi: 10.1126/science.219.4588.1073, 1983.

Thiemens, M. H.: Mass-independent isotope effects in planetary atmospheres and the early solar system, Science, 283, 341-345, doi: 10.1126/science.283.5400.341, 1999.

Turekian, V. C., Macko, S., Ballentine, D., Swap, R. J., and Garstang, M.: Causes of bulk carbon and nitrogen isotope fractionations in the products of vegetation burns: laboratory studies, Chem. Geol., 152, 181-192, doi: 10.1016/S0009-2541(98)00105-3, 1998.

Walters, W. W., Goodwin, S. R., and Michalski, G.: Nitrogen stable isotope composition ($\delta^{15}N$) of vehicle-emitted NO_x, Environ. Sci. Technol., 49, 2278-2285, doi: 10.1021/es505580v, 2015.

Walters, W. W., and Michalski, G.: Theoretical calculation of nitrogen isotope equilibrium exchange fractionation factors for various NO_y molecules, Geochim. Cosmochim. Ac., 164, 284-297, doi: 10.1016/j.gca.2015.05.029, 2015.

Walters, W. W., and Michalski, G.: Theoretical calculation of oxygen equilibrium isotope fractionation factors involving various NO_y molecules, OH, and H_2O and its implications for isotope variations in atmospheric nitrate, Geochim. Cosmochim. Ac., 191, 89-101, doi: 10.1016/j.gca.2016.06.039, 2016.

Walters, W. W., Simonini, D. S., and Michalski, G.: Nitrogen isotope exchange between NO and NO_2 and its implications for $\delta^{15}N$ variations in tropospheric NO_x and atmospheric nitrate, Geophys. Res. Lett., 43, 440-448, doi: 10.1002/2015gl066438, 2016.

© Author(s) 2018. CC BY 4.0 License.

Wang, H., Lu, K., Chen, X., Zhu, Q., Chen, Q., Guo, S., Jiang, M., Li, X., Shang, D., Tan, Z., Wu, Y., Wu, Z., Zou, Q., Zheng, Y., Zeng, L., Zhu, T., Hu, M., and Zhang, Y.: High N_2O_5 concentrations observed in urban Beijing: Implications of a large nitrate formation pathway, Environ. Sci. Technol. Lett., 4, 416-420, doi: 10.1021/acs.estlett.7b00341, 2017.

Wankel, S. D., Chen, Y., Kendall, C., Post, A. F., and Paytan, A.: Sources of aerosol nitrate to the Gulf of Aqaba: Evidence from $\delta^{15}N$ and $\delta^{18}O$ of nitrate and trace metal chemistry, Mar. Chem., 120, 90-99, doi: 10.1016/j.marchem.2009.01.013, 2010.

Wojtal, P. K., Miller, D. J., O'Conner, M., Clark, S. C., and Hastings, M. G.: Automated, high-resolution mobile collection system for the nitrogen isotopic analysis of NO_x, J. Vis. Exp., 118, e54962, doi: 10.3791/54962, 2016.

Yienger, J. J., and Levy, H.: Empirical model of global soil-biogenic NO_x emissions, J. Geophys. Res., 100, 11447-11464, doi: 10.1029/95JD00370, 1995.

Zhang, Q., Geng, G., Wang, S., Richter, A., and He, K.: Satellite remote sensing of changes in NO_x emissions over China during 1996-2010, Chinese Sci. Bull., 57, 2857-2864, doi: 10.1007/s11434-012-5015-4, 2012.

Zhang, R., Tie, X., and Bond, D. W.: Impacts of anthropogenic and natural NO_x sources over the U.S. on tropospheric chemistry, P. Natl. Acad. Sci. U.S.A, 100, 1505-1509, doi: 10.1073/pnas.252763799, 2003.

Zhao, B., Wang, S. X., Liu, H., Xu, J. Y., Fu, K., Klimont, Z., Hao, J. M., He, K. B., Cofala, J., and Amann, M.: NO_x emissions in China: historical trends and future perspectives, Atmos. Chem. Phys., 13, 9869-9897, doi: 10.5194/acp-13-9869-2013, 2013.

Zhao, Y., Qiu, L. P., Xu, R. Y., Xie, F. J., Zhang, Q., Yu, Y. Y., Nielsen, C. P., Qin, H. X., Wang, H. K., Wu, X. C., Li, W. Q., and Zhang, J.: Advantages of a city-scale emission inventory for urban air quality research and policy: the case of Nanjing, a typical industrial city in the Yangtze River Delta, China, Atmos. Chem. Phys., 15, 12623-12644, doi: 10.5194/acp-15-12623-2015, 2015.

Zong, Z., Wang, X., Tian, C., Chen, Y., Fang, Y., Zhang, F., Li, C., Sun, J., Li, J., and Zhang, G.: First assessment of NO_x sources at a regional background site in North China using isotopic analysis linked with modeling, Environ. Sci. Technol., 51, 5923-5931, doi: 10.1021/acs.est.6b06316, 2017.

Atmos. Chem. Phys. Discuss., https://doi.org/10.5194/acp-2018-385
Manuscript under review for journal Atmos. Chem. Phys.
Discussion started: 8 May 2018
© Author(s) 2018. CC BY 4.0 License.

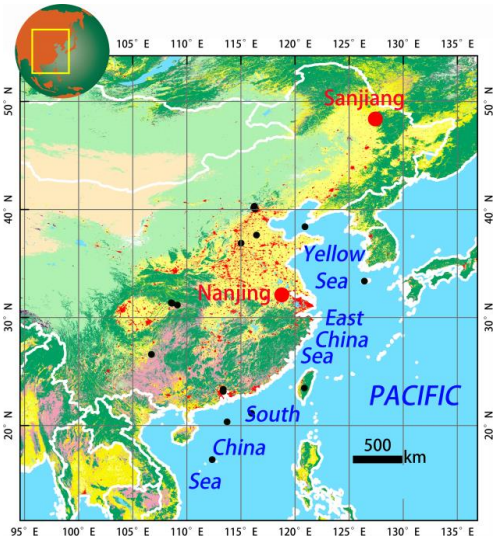

Figure 1. Location of the sampling sites Sanjiang and Nanjing. The black dots indicate the location of sampling sites (sites are located in the area of mainland China and the Yellow and East and South China Seas) with $\delta^{15}N\text{-}NO_3^-$ data from the literature (see also Table S4).

Atmos. Chem. Phys. Discuss., https://doi.org/10.5194/acp-2018-385
Manuscript under review for journal Atmos. Chem. Phys.
Discussion started: 8 May 2018
© Author(s) 2018. CC BY 4.0 License.

Atmospheric Chemistry and Physics Discussions

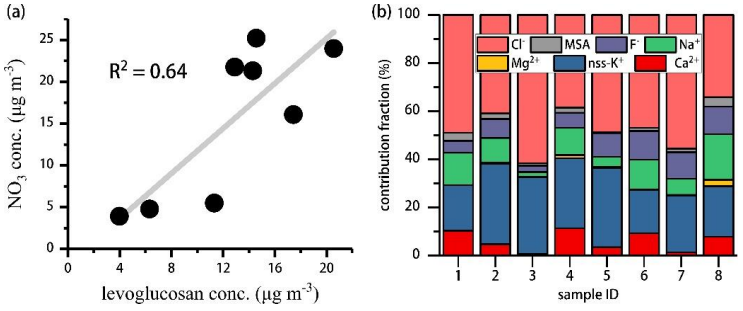

Figure 2. (**a**) Correlation analysis between the mass concentrations of levoglucosan and aerosol nitrate during the Sanjiang sampling campaign; (**b**) Variation of fractions of various inorganic species during day-night samplings at Sanjiang between 8 and October 2013 18 (sample ID 1 to 8, respectively). The higher relative abundances of nss-K^+ and Cl^- are indicative for a biomass-burning dominated source. For sample ID information and exact sampling dates, refer to Table S3.

Atmos. Chem. Phys. Discuss., https://doi.org/10.5194/acp-2018-385
Manuscript under review for journal Atmos. Chem. Phys.
Discussion started: 8 May 2018
© Author(s) 2018. CC BY 4.0 License.

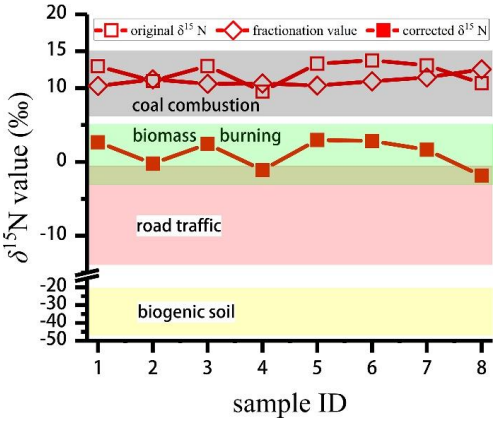

Figure 3. Original $\delta^{15}N$ values ($\delta^{15}N_{ini}$) for pNO_3^-, calculated values for the N isotope fractionation (ε_N) associated with the conversion of gaseous NO_x to pNO_3^-, and corrected $\delta^{15}N$ values ($\delta^{15}N_{corr}$; $^{15}N_{ini}$ minus ε_N) of pNO_3^- for each sample collected during the Sanjiang sampling campaign. The colored bands represent the variation range of $\delta^{15}N$ values for different NO_x sources based on reports from the literature (Table S2). See Table S3 for the information regarding sample ID.

Atmos. Chem. Phys. Discuss., https://doi.org/10.5194/acp-2018-385
Manuscript under review for journal Atmos. Chem. Phys.
Discussion started: 8 May 2018
© Author(s) 2018. CC BY 4.0 License.

Atmospheric Chemistry and Physics Discussions

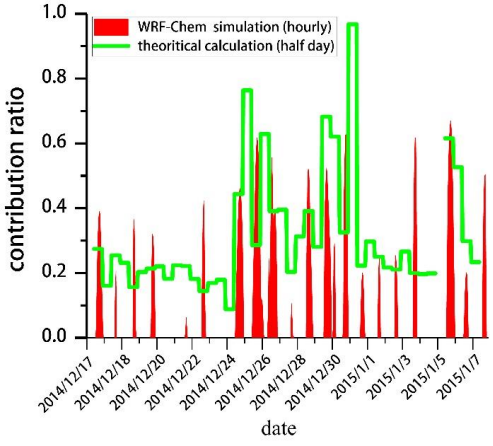

935

936 **Figure 4**. Comparison between the theoretical calculation and WRF-Chem simulation
937 of the average contribution ratio (γ) for nitrate formation in Nanjing via the reaction
938 of NO_2 and photochemically produced •OH.

939

940

941

942

Atmos. Chem. Phys. Discuss., https://doi.org/10.5194/acp-2018-385
Manuscript under review for journal Atmos. Chem. Phys.
Discussion started: 8 May 2018
© Author(s) 2018. CC BY 4.0 License.

Atmospheric Chemistry and Physics Discussions

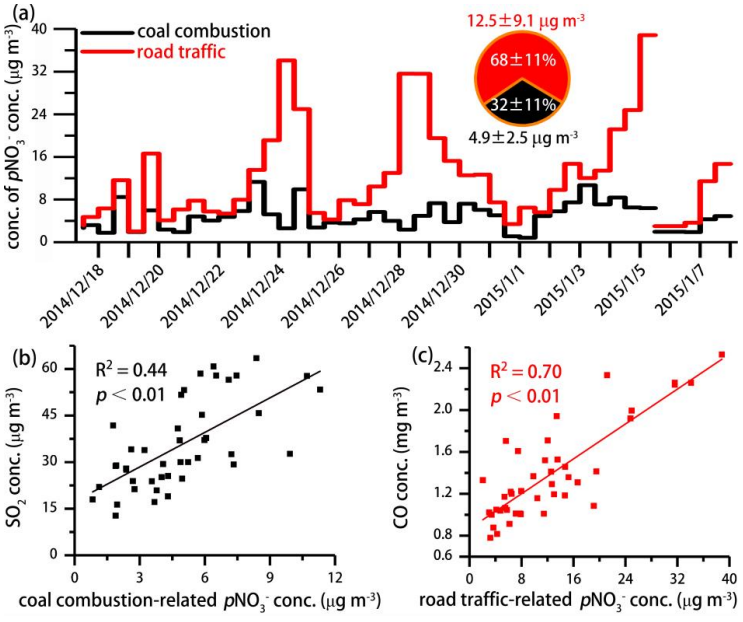

Figure 5. (**a**) Time-series variation of coal combustion and road traffic contribution to the mass concentrations of ambient pNO_3^- in Nanjing, as estimated through MixSIR; (**b**) Correlation analysis between the mass concentrations of coal combustion-related pNO_3^- and SO_2; (**c**) Correlation analysis between the mass concentrations of road traffic-related pNO_3^- and CO.

Atmos. Chem. Phys. Discuss., https://doi.org/10.5194/acp-2018-385
Manuscript under review for journal Atmos. Chem. Phys.
Discussion started: 8 May 2018
© Author(s) 2018. CC BY 4.0 License.

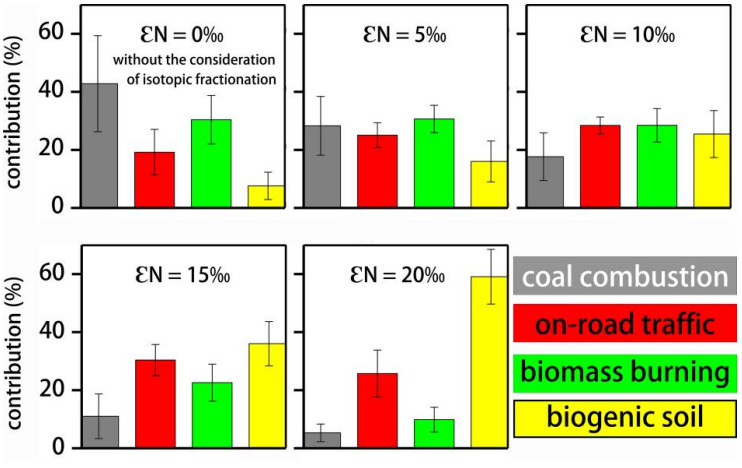

Figure 6. Estimates of the relative importance of single NO_x sources (mean ± 1σ) throughout China based on the original $\delta^{15}N\text{-}NO_3^-$ values extracted from the literature (ε_N = 0‰) and under consideration of significant N isotope fractionation during NO_x transformation (ε_N = 5‰, 10‰, 15‰ or 20‰).